



THE UNIVERSITY *of* EDINBURGH

## Edinburgh Research Explorer

# The electronic states of 1,2,4-triazoles: A study of 1H- and 1-methyl-1,2,4-triazole by vacuum ultraviolet photoabsorption and ultraviolet photoelectron spectroscopy and a comparison with ab initio configuration interaction computations

### Citation for published version:

Palmer, MH, Camp, PJ, Hoffmann, SV, Jones, NC, Head, AR & Lichtenberger, DL 2012, 'The electronic states of 1,2,4-triazoles: A study of 1H- and 1-methyl-1,2,4-triazole by vacuum ultraviolet photoabsorption and ultraviolet photoelectron spectroscopy and a comparison with ab initio configuration interaction computations', *The Journal of Chemical Physics*, vol. 136, no. 9, 094310, pp. -. <https://doi.org/10.1063/1.3692164>

### Digital Object Identifier (DOI):

[10.1063/1.3692164](https://doi.org/10.1063/1.3692164)

### Link:

[Link to publication record in Edinburgh Research Explorer](#)

### Document Version:

Publisher's PDF, also known as Version of record

### Published In:

The Journal of Chemical Physics

### Publisher Rights Statement:

Copyright 2012 American Institute of Physics. This article may be downloaded for personal use only. Any other use requires prior permission of the author and the American Institute of Physics.

### General rights

Copyright for the publications made accessible via the Edinburgh Research Explorer is retained by the author(s) and / or other copyright owners and it is a condition of accessing these publications that users recognise and abide by the legal requirements associated with these rights.

### Take down policy

The University of Edinburgh has made every reasonable effort to ensure that Edinburgh Research Explorer content complies with UK legislation. If you believe that the public display of this file breaches copyright please contact [openaccess@ed.ac.uk](mailto:openaccess@ed.ac.uk) providing details, and we will remove access to the work immediately and investigate your claim.



**The electronic states of 1,2,4-triazoles: A study of 1H- and 1-methyl-1,2,4-triazole by vacuum ultraviolet photoabsorption and ultraviolet photoelectron spectroscopy and a comparison with ab initio configuration interaction computations**

Michael H. Palmer, Philip J. Camp, Søren Vrønning Hoffmann, Nykola C. Jones, Ashley R. Head et al.

Citation: *J. Chem. Phys.* **136**, 094310 (2012); doi: 10.1063/1.3692164

View online: <http://dx.doi.org/10.1063/1.3692164>

View Table of Contents: <http://jcp.aip.org/resource/1/JCPSA6/v136/i9>

Published by the [AIP Publishing LLC](#).

---

**Additional information on J. Chem. Phys.**

Journal Homepage: <http://jcp.aip.org/>

Journal Information: [http://jcp.aip.org/about/about\\_the\\_journal](http://jcp.aip.org/about/about_the_journal)

Top downloads: [http://jcp.aip.org/features/most\\_downloaded](http://jcp.aip.org/features/most_downloaded)

Information for Authors: <http://jcp.aip.org/authors>

**ADVERTISEMENT**



Explore the **Most Cited**  
Collection in Applied Physics

**AIP**  
Publishing

# The electronic states of 1,2,4-triazoles: A study of 1H- and 1-methyl-1,2,4-triazole by vacuum ultraviolet photoabsorption and ultraviolet photoelectron spectroscopy and a comparison with *ab initio* configuration interaction computations

Michael H. Palmer,<sup>1,a)</sup> Philip J. Camp,<sup>1,b)</sup> Søren Vrønning Hoffmann,<sup>2,c)</sup>  
Nykola C. Jones,<sup>2,d)</sup> Ashley R. Head,<sup>3</sup> and Dennis L. Lichtenberger<sup>3,e)</sup>

<sup>1</sup>*School of Chemistry, University of Edinburgh, West Mains Road, Edinburgh EH9 3JJ, Scotland, United Kingdom*

<sup>2</sup>*Institute for Storage Ring facilities (ISA), Department of Physics and Astronomy, Aarhus University, Ny Munkegade 120, Building 1520, DK-8000 Aarhus C, Denmark*

<sup>3</sup>*Department of Chemistry and Biochemistry, The University of Arizona, Tucson, Arizona 85721, USA*

(Received 3 October 2011; accepted 16 February 2012; published online 7 March 2012)

The first vacuum ultraviolet absorption spectrum of a 1,2,4-triazole has been obtained and analyzed in detail, with assistance from both an enhanced UV photoelectron spectroscopic study and *ab initio* multi-reference multi-root configuration interaction procedures. For both 1H- and 1-methyl-1,2,4-triazoles, the first ionization energy bands show complex vibrational structure on the low-energy edges of otherwise unstructured bands. Detailed analysis of these bands confirms the presence of three ionized states. The 6–7 eV VUV spectral region shows an unusual absorption plateau, which is interpreted in terms of the near degeneracy of the first two ionization energies, leading to a pseudo Jahn-Teller effect. The “fingerprint” of the ionization spectrum yields band origins for several Rydberg states. The configuration interaction study shows that although the equilibrium structure for the first cation is effectively planar, the second cation shows significant twisting of the ring system. Some calculated singlet electronic states also show skeletal twisting in which the ring C–H is substantially out of plane. © 2012 American Institute of Physics. [<http://dx.doi.org/10.1063/1.3692164>]

## I. INTRODUCTION

1,2,4-triazole (**1H124T**, Fig. 1) is an historically important heterocyclic compound with diverse biological properties; thus derivatives occur in various commercial products, including antiviral, antibacterial, antifungal, herbicidal, hypnotic, and antiasthmatic drugs.<sup>1</sup> Recently, its high binding affinity for various cytochrome P450 proteins has led to use in positron emission tomography to target aromatase, an important enzyme in human tumors<sup>2</sup> and other living matter. Spectroscopic study of the ground and excited electronic state structures for 1,2,4-triazoles are few, especially in the vacuum ultraviolet (VUV) and ionization energy regions. **1H124T** shows low vapor pressure for gaseous spectroscopic analysis at ambient temperature under synchrotron conditions; *N*-methylation to the molecule to **1Me124T** (Fig. 1) increases the volatility markedly and has enabled us to obtain the VUV spectrum. Recently we demonstrated the synergistic value of VUV absorption spectroscopy and ultraviolet photoelectron spectroscopy (UPS)<sup>3</sup> for the related compound 2H-1,2,3-triazole (**2H123T**). The interconnection of UPS with VUV photoabsorption spectra arises through Rydberg states. The vibrational pattern (“footprint”) in the UPS is expected to be

present in Rydberg states in the VUV spectrum; since the excited electron becomes distant from the nuclei, its potential is similar to that for ionization. Hence these footprints are critical in locating Rydberg states in VUV spectra. A number of ionic and singlet excited electronic states have been identified, and their equilibrium structures investigated computationally. We will see that non-planar skeletal twisting occurs for several of the low energy ionized and excited states.

We have re-determined the UPS spectra of **1H124T** and **1Me124T** under much higher resolution than previous studies, which were focused on the position of the tautomeric 1H versus 4H atoms (Fig. 1).<sup>4</sup> These new spectra have enabled adiabatic ionization energies (IE<sup>A</sup>) and Rydberg absorption band origins to be determined. The study of molecular Rydberg states occupies an important place in molecular spectroscopy,<sup>5–7</sup> and comprehensive accounts of their properties, particularly for low-lying Rydberg states with principal quantum number  $n < 20$ , have been given.<sup>8–11</sup> Furthermore, electronic excitations and Rydberg states of molecules are fundamental to many molecular properties and remain active areas of research for experimentalists and theoreticians.<sup>12–21</sup> The Rydberg states have term values given by

$$\text{Term value} = \text{IE} - E_n = \frac{R}{(n - \delta)^2}, \quad (1)$$

where IE is the ionization energy,  $E_n$  is the  $n$ -th energy level,  $R$  is the Rydberg constant, and  $\delta$  is the quantum defect. **1Me124T** is a suitable derivative to study the

<sup>a)</sup>Telephone: +44 (0) 131 650 4765. Fax: +44 (0) 131 650 6453. Electronic mail: m.h.palmer@ed.ac.uk.

<sup>b)</sup>Electronic mail: philip.camp@ed.ac.uk.

<sup>c)</sup>Electronic mail: vronning@phys.au.dk.

<sup>d)</sup>Electronic mail: nykj@phys.au.dk.

<sup>e)</sup>Electronic mail: dlichten@email.arizona.edu.

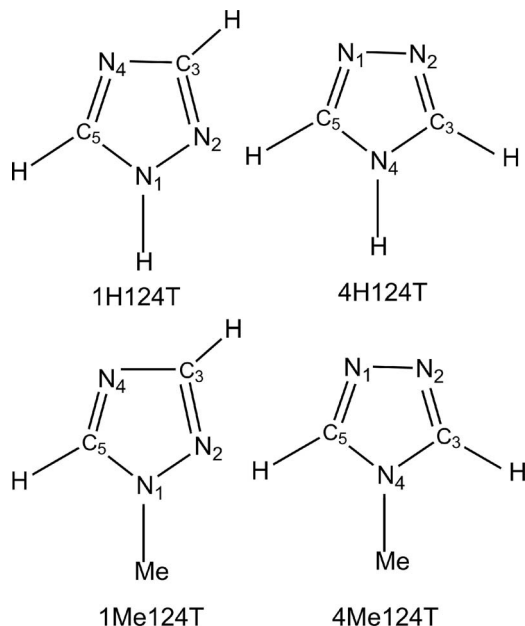


FIG. 1. The compounds under study, **1H124T** and **1Me124T**, and their isomers.

intrinsic properties of the **1H124T** system since microwave spectroscopy (MW),<sup>22–24</sup> electron diffraction (ED),<sup>25</sup> and UPS investigations<sup>4</sup> identified only the 1H-tautomer in the gas phase. Equilibrium structures for the pair of **124T** tautomers at the configuration interaction (CI) level<sup>26</sup> lead to the same conclusion.

## II. EXPERIMENTAL AND COMPUTATIONAL DETAILS

### A. Experimental

**1Me124T** was prepared from **1H124T** (Sigma-Aldrich) by methylation using iodomethane. The photoabsorption spectrum of **1Me124T** was taken using the UV1 beamline on the ASTRID storage ring at Aarhus University, Denmark, as described previously.<sup>3</sup> The gas cell and the sample container were held at 30°C during measurements. The He I and He II UPS for **1H124T** and **1Me124T**, recorded with an instrument and methods described previously,<sup>3,28–30</sup> had significantly higher resolution than in previous studies.<sup>4</sup> **1H124T** sublimed at 25°C–31°C; **1Me124T** was introduced into the vacuum system at ambient temperature from a Young's tube via a needle valve. Both samples showed evidence of water contamination (12.62 eV), which was subtracted from the spectral data for clarity. Further details of the sample characterization and these two spectroscopies are given in the supplemental material.<sup>27</sup>

### B. Computational details

*Ab initio* calculations were performed with the GAMESS-UK,<sup>31</sup> GAUSSIAN-09,<sup>32</sup> and MOLPRO<sup>33,34</sup> suites of programs. The main vertical excitation study of the VUV spectrum of **1Me124T** used the multi-reference multi-root doubles and singles method (MRD-CI) as discussed below; the cc-pVTZ basis set<sup>35</sup> containing C,N(10s5p2d1f) and H(5s,3p2d1f)

atomic orbitals contracted to [4s3p2d1f]/[3s2p1d] (total of 199AOs), was augmented by *s,p,d,f*-Rydberg state exponents [4s3p3d3f] at the center of mass, as given previously.<sup>3,36</sup> Most excited state structures were determined with a TZVP basis set of atomic orbitals, C,N(11s6p1d) contracted to C,N(5s3p1d)<sup>37</sup> since this allows additional flexibility in the valence space when compared with cc-pVTZ through more valence and fewer polarization functions. The methodology used was restricted open shell Hartree-Fock (ROHF) together with singles + doubles CI (SDCI). Techniques for determining the individual structures are described in the supplemental material.<sup>27</sup> Plotting and fitting of the present data used ORIGIN 8,<sup>38</sup> GNU PLOT,<sup>39</sup> and Visual Molecular Dynamics (VMD).<sup>40</sup>

### 1. Multi-reference multi-root configuration interaction calculations

The main VUV study was performed with a version of the MRD-CI<sup>41–43</sup> module embedded in the GAMESS-UK code;<sup>31</sup> this includes *f*-orbital and *f*-electronic state capability. The calculations were performed at the corresponding  $\tilde{X}^1A_1$  ground state equilibrium geometry, and the 32 valence electrons, together with the lowest 170 virtual orbitals were active. For simplicity in the discussion of Rydberg states, we denote  $p_x$ ,  $d_{xz}$ , and  $f_{xxx}$  states as X, XZ, XXX etc., while XX etc. is used instead of  $X^2$ . The procedure is described in greater detail in Ref. 3. The theoretical oscillator strengths  $f(r)$  usually enable differentiation between valence and Rydberg states, for which values of  $f(r)$  are typically  $10^{-1}$ – $10^{-2}$  and  $10^{-2}$ – $10^{-6}$ , respectively. In the present study with **1Me124T**, the oscillator strengths were determined from CI wavefunctions within the MRD-CI module.<sup>41–43</sup>

## III. COMPUTATIONAL RESULTS FOR THE NEUTRAL MOLECULES AND LOWEST POSITIVE ION STATES

### A. The molecular structures of **1H124T** and **1Me124T** in their ground, singlet excited, and cationic states

#### 1. Ground state structure comparison with experiment

Experimental gas phase MW<sup>22–24</sup> and ED studies<sup>25</sup> for **1H124T** have been reported, but with both studies there are insufficient data for independent determination of all structural parameters. Some of the tentative MW structural results<sup>22–24</sup> were based upon related compounds. The ED study<sup>25</sup> is problematic because of the difficulty in obtaining unique results for a molecule with four CN bond distances of similar magnitude. However, the rotational constants (**A**,**B**,**C**) for **1H124T** are unambiguous at **A** = 10.245, **B** = 9.832, and **C** = 5.015 GHz, respectively;<sup>24</sup> the present SDCI optimized structure (Fig. 2) gives **A** = 10.477, **B** = 10.065, and **C** = 5.133 GHz, about 2% larger than experiment. The cc-pVTZ self-consistent field (SCF) equilibrium structure gives even larger values of **A** = 10.553, **B** = 10.232, and **C** = 5.195 GHz, respectively. The experimental dipole moment (DM) ( $\mu$  = 2.7 D)<sup>24</sup> is also smaller than both the present SDCI value

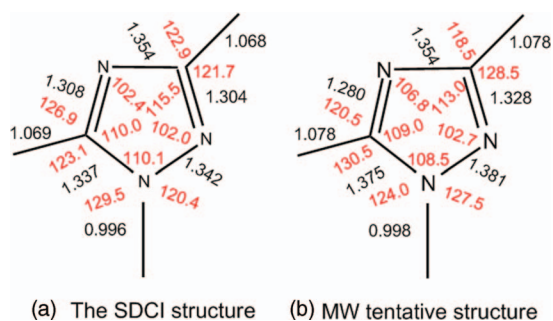


FIG. 2. The ground state structure (Å and °) from the SDCI theoretical study (a) compared with the provisional microwave structure study<sup>24</sup>(b).

$\mu = 3.07$  D and cc-pVTZ value  $\mu = 3.12$  D. The structural parameters for the SDCI optimized study are relatively close to those suggested from the MW study<sup>24</sup> (Fig. 2); the internal ring angles are typical, with the sequence of magnitudes  $C_3 > C_5 \sim N_1 > N_4 > N_2$ . Both the experimental<sup>22–25</sup> and theoretical (Fig. 2) bond distances reflect the classical representation of alternating single and double bonds. In the  $-N_2 = C_3 - N_4 = C_5 - N_1 -$  ring unit, the  $N_2C_3$  and  $N_4C_5$  bonds are short. For the present purposes, these calculated values are sufficiently close to experiment, and we will concentrate upon the (larger) calculated differences with electronic states below.

The conformation of the methyl group in *IMe124T*, studied by variation of the torsion angle  $H_1C_1N_1N_2$  ( $\theta$ ), shows that the lowest energy conformer has  $\theta = 180^\circ$ , and this is used for study of the vertical ionization. The calculated internal rotation barrier is  $236 \text{ cm}^{-1}$ . The MW determined barriers for *N*-methyl-derivatives of pyrrole and pyrazole are somewhat lower ( $54$  and  $44 \text{ cm}^{-1}$ , respectively).<sup>44</sup> There is no gas phase experimental structural material for *IMe124T*, but crystal structures of several substituted versions of *IMe124T* are known,<sup>45</sup> in which the methyl group also shows  $H_1C_1N_1N_2 = 180^\circ$ .

## 2. Excited electronic state structures

The classical ground state representation of the ring unit with short  $N_2C_3$  and  $N_4C_5$  bonds mentioned previously does not occur for several excited electronic and ionic states for *IMe124T*. Several excited states are non-planar ( $1^2A$  to  $3^2A$ ), as is the second ionic state ( $1^2A$ , notionally  $2^2A''$ ), and in these cases internal rotation of the methyl group is also observed. A series of planar and non-planar equilibrium structures for each type is shown in the supplemental material<sup>27</sup> (Figs. S1–S4).

It proved impossible to generate a non-planar version of the lowest vertical state  $1^1A''$ . This state seems properly represented by the planar  $18a'5a''$  structure in Fig. S3. However, non-planar structures were found as minima on the potential energy surfaces for other excited states. Owing to the difficulty in obtaining comparable ground state energies for the optimized non-planar open shell singlet states, a feature of the very different levels of electron correlation, the following excitation energies (EE) are relative energies. The excita-

tions are best described by their unique structural features and the dipole moments, which vary considerably. In most cases studied, the methyl group rotates from the ground state ( $C_s$ ) such that one H atom ( $H_A$ ) is pointing nearly perpendicular to the mean triazole plane.

The lowest energy non-planar singlet state  $1^1A$  structure (structure A, Fig. S4), with relative EE  $4.45$  eV and DM  $1.7$  D, has  $H_5$  strongly out-of-plane and is *cis* with respect to  $H_A$  of the methyl group. The  $2^1A$  singlet (structure B, Fig. S4) is close by with relative EE at  $4.67$  eV but has an even larger DM of  $3.1$  D. This state has  $H_3$  strongly out-of-plane and *trans* to  $H_A$ . The electron distributions for these two states show highest electron density perpendicular to the mean ring atom plane. Hence, both are effectively distorted versions of the planar  $1^1A'$  and  $2^1A'$  states. Indeed, these last two states have closely related structures, which show that the vertical excitations to the planar  $1^1A'$  ( $4a''5a''$ ) and  $2^1A'$  ( $3a''5a''$ ) states are a coupled pair, and hence behave as a pseudo degenerate system; this will be significant for the discussion of the complexity of the  $6\text{--}7$  eV region of the VUV spectrum. The principal densities in  $1^1A$  and  $2^1A$  are relatively close to those of the  $1^1A''$  and  $2^1A'$  states. This makes it convenient to retain the  $C_s$  symmetry designations in later discussions.

## 3. Cationic state structures

The ionic states in the supplemental material<sup>27</sup> show similar effects. The distinct character of  $1^2A''$  and  $2^2A''$  states is obvious; lengthening of a bond in one cation, leads to shortening for the other cation at both the ROHF and SDCI levels (Figs. S1 and S2). When deviations from planarity are considered, the effects of the  $1^2A'$  change to  $1^2A$  are relatively small, with a maximum twisting of the  $H_1C_1N_1C_5$  dihedral angle by  $3.7^\circ$  (Fig. S2). Comparison of  $2^2A''$  to  $2^2A$  shows much larger deviations from planarity, with the  $N_2C_3N_4C_5$  dihedral angle twisted by  $12.3^\circ$ . In addition,  $C_3$  and  $C_5$  move to one side of the mean plane of the ring while  $N_2$  and  $N_4$  move to the other side. However, the  $1^2A$  and  $2^2A$  wavefunctions clearly show the predominant  $A''$  nature of both these states.

## B. Calculated ionic state energies of *1H124T* and *1Me124T* in relation to the UPS spectra

### 1. Relative energy considerations

Initial equilibrium ionic structure studies of *IMe124T* showed that  $2^2A''$  and  $1^2A''$  ( $3a''^{-1}$  and  $4a''^{-1}$ ) have a small energy difference varying from  $0.41$  eV (B3LYP) to  $0.44$  eV (ROHF) to  $0.51$  eV (SDCI). When the structures were allowed to become non-planar ( $C_1$ ), a very similar SDCI energy difference ( $0.41$  eV) was obtained for the corresponding  $2^2A$  and  $1^2A$  states, but the structures of these cations, shown in the supplemental material<sup>27</sup> (Figs. S1 and S2), are significantly different.  $1^2A$  is effectively indistinguishable from  $1^2A''$ ;  $2^2A$  is significantly non-planar, but still shows a relatively close relationship to  $2^2A'$ . It is convenient to refer to these two states as  $1^2A''$  and  $2^2A''$ , ignoring the non-planarity of  $2^2A''$ . In this representation the four lowest ionic states consist of two  $\pi$ -ionizations ( $1^2A''$  and  $2^2A''$ ) and two  $\sigma$ -ionizations ( $1^2A'$  and

$2^2A'$ ), as have been discussed previously for *1H124T*.<sup>46</sup> The most important MOs in the theoretical study of *1Me124T* are shown in the supplemental material<sup>27</sup> (Fig. S5).

## 2. Frequencies

The lowest calculated anharmonic vibrational frequency for *1Me124T*, using the B3LYP method, is  $82\text{ cm}^{-1}$ , a value consistent with the methyl torsional mode in *N*-methylpyrrole ( $54\text{ cm}^{-1}$ ).<sup>44</sup> Unfortunately, we are unable to calculate anharmonic vibration frequencies at the SDCl level, although the restricted active space self-consistent field (RASSCF) method of MOLCAS allows a limited CI approach. We developed a correlation between our harmonic and anharmonic frequencies where both sets are available for the  $1^2A''$  and  $1^2A'$  cations at the ROHF level; this allows us to convert our harmonic frequencies into “anharmonic” frequencies. The frequencies were found to exhibit a close linear correlation:  $\nu_{\text{anharmonic}} = [0.969(5)\nu_{\text{harmonic}} + 2(9)]\text{ cm}^{-1}$ , with a correlation coefficient  $R^2 = 0.999$ . We ignore the intercept, and the “anharmonic” frequencies below have been obtained by scaling the harmonic frequencies by 0.969.

The intensities of the UPS ionizations, discussed below, are related to the dipole moment operator between the neutral and positive ion electronic states and the overlap integral between the vibrational levels. Here, we perform a superposition of the calculated ionic state frequencies and intensities onto the UPS Band 1 moiety. An example of the success of this procedure is shown in the supplemental material<sup>27</sup> (Fig. S7) for the UPS Band 1 of the furan molecule.

## IV. UPS RESULTS

### A. UPS assignments for the *1H124T* and *1Me124T* full valence region

The experimental photoelectron spectra are shown in Fig. 3 and illustrate our theoretical study using the Tamm-Dancoff approximation (TDA) in comparison to the experimental spectra.<sup>47</sup> This computational method has the widest energy range with intensities available to us, and includes “shake-up state” solutions. Various experimental and computational determinations of the adiabatic and vertical ionization energies are collected in Table I. Some of these UPS results confirm early studies for both *1H124T*<sup>47</sup> and *1Me124T*.<sup>4</sup> The lowest cationic state is  $1^2A''$  for both molecules. Comparison of the UPS (Fig. 3) shows that the two spectra are very similar up to 12 eV as expected.<sup>48</sup> For *1H124T* this consists of ionizations  $1^2A'' < 2^2A'' < 1^2A'$  ( $15a'^{-1}$ ,  $LP_{N4}$ )  $< 2^2A'$  ( $14a'^{-1}$ ,  $LP_{N2}$ ) (Table I). The additional band near 14.5 eV for *1Me124T* contains methyl group ionization ( $3^2A'$  and  $3^2A''$ ), with the remaining two peaks in the 15–16 eV region being  $4^2A'$ ,  $5^2A'$ , and  $4^2A''$ . The TDA calculations suggest that all MOs up to  $\sim 18$  eV give ionic states dominated by one-electron processes. Above this energy, the splitting of density into several ionic states is visible (Fig. 3). Some examples are noted in the supplemental material<sup>27</sup> (Table S1).

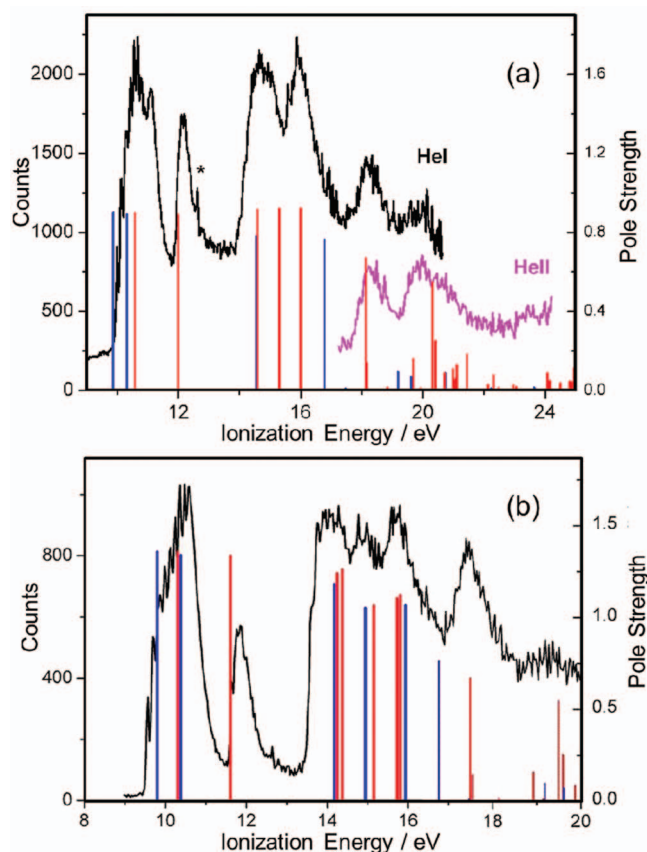


FIG. 3. UPS spectra for the outer valence region of (a) *1H124T* and (b) *1Me124T*. The energies and pole strengths of ionizations calculated by the Tamm-Dancoff approximation are shown as vertical bars, where blue bars show  $\pi$ -ionizations and the red bars show  $\sigma$ -ionizations.

### B. Vibrational structure in the UPS spectra for *1H124T* and *1Me124T*

The first ionization bands (Fig. 4) show a complex envelope where the low-energy side (leading edge) consists of a series of maxima on a rising background; these are detailed in the supplemental material<sup>27</sup> (Table S2). This vibrational structure is superimposed on a broad background peak at the high-energy end, which is most evident in the spectrum of *1H124T* (Fig. 4(a)). Each spectrum shows a low intensity 0-0 band ( $IE^A$ ), giving the adiabatic  $IE_1^A$  as 9.99 (*1H124T*) and 9.57 eV (*1Me124T*), respectively. The peak widths are equivalent to the spectrometer resolution. The separation of the subsequent maxima decreases, in *1Me124T* (Fig. 4(b)) from 0.15 eV (at 9.71 eV) to 0.11 eV (at 10.59 eV). The peak width increase with increasing energy; for *1Me124T* the second maximum (9.71 eV) is broader than the first, while the third maximum (9.85 eV) is nearly double in width compared with the other bands, and the fourth maximum also shows a subsidiary peak. This structure suggests a complex manifold of overlapping vibrational progressions, and this is further indicated by the frequencies obtained from the deconvolution in Sec. IV C. The high energy sides (trailing edges) of both *1H124T* and *1Me124T* show no discernable fine structure at this resolution.

TABLE I. Selected ionization energies from the UV photoelectron data and calculations of 1H- and 1-methyl-1,2,4-triazole with different methods (all energies in eV).

| Expt. IE<br>(eV)        | Fitted IE <sup>a</sup><br>(eV) | Symmetry and open<br>shell vacancy | MRD-CI        | TDA           | GF    |       |
|-------------------------|--------------------------------|------------------------------------|---------------|---------------|-------|-------|
| 1H-1,2,4-triazole       |                                |                                    |               |               |       |       |
| (A or V)                | Calculated IE                  | $c_i^2$                            | Calculated IE | Calculated IE |       |       |
| 9.99A                   | 9.989(2)                       | 3a''                               | 9.84          | 0.85          | 9.65  | 9.69  |
| 10.56V                  | 10.222(2)                      | 2a''                               | 10.72         | 0.84          | 10.32 | 10.27 |
| 11.09V                  | 11.165(6)                      | 15a'                               | 9.90          | 0.83          | 11.11 | 10.89 |
| 12.16V                  | 11.987(2)                      | 14a'                               | 11.34         | 0.83          | 12.50 | 12.34 |
| 1-methyl-1,2,4-triazole |                                |                                    |               |               |       |       |
| 9.57A                   | 9.576(2)                       | 4a''                               | 9.56          | 0.84          | 10.22 | 9.79  |
|                         | 9.887(3)                       | 3a''                               | 10.21         | 0.83          | 10.85 | 10.37 |
|                         | 10.574(6)                      | 12a'                               | 10.31         | 0.84          | 10.57 | 10.62 |
| 11.63V                  | 11.632(2)                      | 11a'                               | 11.64         | 0.83          | 11.88 | 12.21 |

<sup>a</sup>Fitted IE from analysis of UPS spectrum; for further details see text and supplemental material.<sup>27</sup>

### C. Deconvolution of the ionization bands of 1H124T and 1Me124T

The three ionizations (two A'' and one A') which occur under the first ionization band for each molecule (Fig. 4) were modelled using a combination of two series of evenly spaced Gaussian functions with Poisson distributed weights,<sup>49</sup> and a further Gaussian which represents the broad trailing edge structure; all of these were superimposed on a linearly increasing background. The most general fitting function of the intensity  $I(E)$  as a function of energy  $E_{\min} \leq E \leq E_{\max}$  that we

used is given by

$$\begin{aligned}
 I(E) = & I_0 + \Delta I_0 \left( \frac{E - E_{\min}}{E_{\max} - E_{\min}} \right) \\
 & + \sum_{k=1}^2 I_k \sum_{v=0}^9 \frac{S_k^v}{v!} \exp \left[ -S_k - \left( \frac{E_k + v\Delta E_k - E}{w_k} \right)^2 \right] \\
 & + I_3 \exp \left[ -\left( \frac{E_3 - E}{w_3} \right)^2 \right], \quad (2)
 \end{aligned}$$

where  $k$  labels the series and  $v$  ( $= 0, 1, 2, \dots, 9$ ) is the vibrational quantum number. For series  $k = 1$  and  $k = 2$ ,  $I_k$  is the intensity,  $S_k$  is the dimensionless Huang-Rhys factor,  $E_k$  is the apparent adiabatic ionization energy for the state,  $\Delta E_k$  is the vibrational energy spacing (assuming a harmonic oscillator and a single vibrational mode progression for each state), and  $w_k$  is a width parameter (assumed equal for each value of  $v$ ). Note that the  $k = 0$  "series" represents the linearly increasing baseline. No vibrational structure is being included in the  $k = 3$  "series," this being characterized only by the intensity  $I_3$ , vertical ionization energy  $E_3$ , and width parameter  $w_3$ .

Figure 4 shows the experimental UPS data and the fitted functions of 1H124T and 1Me124T based on Eq. (2); the complete numerical "fit" parameters are given in Table S3 in the supplemental material,<sup>27</sup> as is a similar analysis of the second ionization band in the region near 12 eV. The fitted  $E_k$  values, listed in Table I, are the adiabatic ionization energies to each different electronic state in this model. The uncertainties shown in parentheses on these energies in Table I represent the variability of the least squares fit model and are not the accuracy of the derived adiabatic ionization energies. For both compounds, these three IE are assigned to  $1^2A''$  ( $\pi$ ),  $2^2A''$  ( $\pi$ ), and  $1^2A'$  ( $\sigma$ ) ionizations, bearing in mind that the structural distortion calculated for the  $IE_2^A$  ionization is more correctly labeled  $1^2A$ . The vibrational frequencies for  $IE_1^A$  and  $IE_2^A$  from the fitting of Band 1 are 1095 and 899  $\text{cm}^{-1}$  for 1H124T, and 985 and 937  $\text{cm}^{-1}$  for 1Me124T; these do not correspond closely to any of the most intense calculated values for harmonic, or derived "anharmonic" frequencies, for

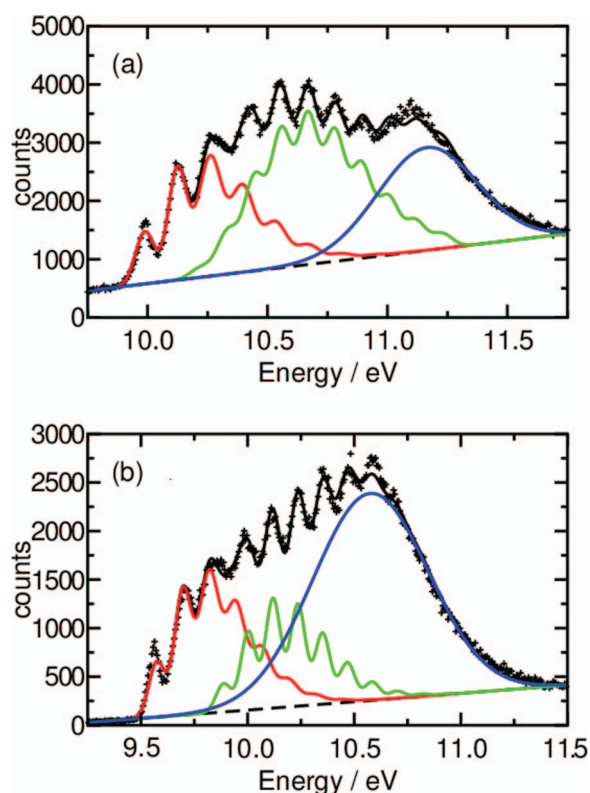


FIG. 4. Expansion of Band 1 of the UPS spectrum of (a) 1H124T and (b) 1Me124T with the superimposed model "fit" (black line) as described in the text.

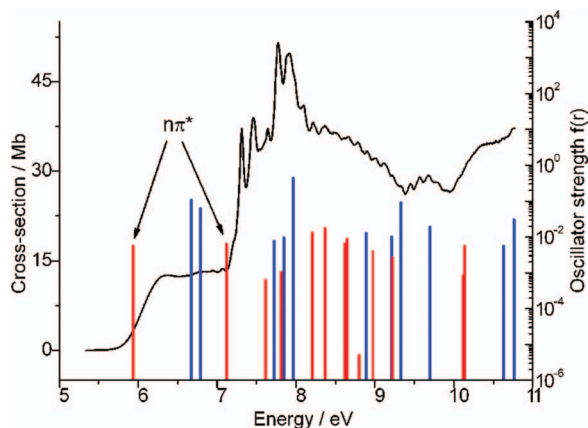


FIG. 5. Calculated valence states superimposed on the VUV spectrum for *1Me124T*. The red bars are calculated  $n\pi^*$   $A'$  states and the blue bars are calculated  $\pi\pi^*$   $A'$  states.

either of the ions, from any of the SDCI, ROHF, or B3LYP methodologies. This strongly suggests that the “fitted” values obtained from the observed spectra, arise from the convolution of several vibrational frequencies in each case.

To further investigate this aspect, we have examined the superposition of calculated ionic state fundamental vibrations on the Band 1 intensity profile similar to the study of furan<sup>50</sup> mentioned previously. Superposition of the calculated frequencies together with intensities for each of the two lowest electronic cationic states (separated in energy according to the SDCI calculations) accounts well for the broadening of the second and third peaks above the ionization onset due to overlap of several vibrational states (supplemental material<sup>27</sup> Fig. S8). The uncertainty increases with higher vibrational quanta, and attempts to generate an envelope from the “stick” diagram intensities to match further details of the experimental spectrum were unproductive.

## V. UV+VUV PHOTOABSORPTION SPECTRUM OF *1Me124T*

The full VUV spectrum with superimposed calculated valence and Rydberg states are shown in Figs. 5 and 6, respectively. The vertical excitation energies and state char-

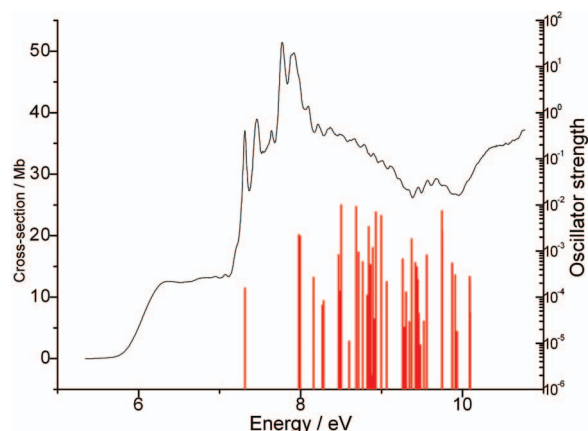


FIG. 6. The calculated Rydberg states superimposed on the VUV spectrum for *1Me124T*.

TABLE II. Selected singlet valence states for 1-methyl-1,2,4-triazole; vertical excitation energies (eV), oscillator strengths, and second moments (a.u.).<sup>a,b,c</sup>

| Energy (eV) | 10 <sup>6</sup> f(r) | Symmetry | State ( $c_i^2 > 0.1e$ ) | $\langle x^2 \rangle$ | $\langle y^2 \rangle$ | $\langle z^2 \rangle$ |
|-------------|----------------------|----------|--------------------------|-----------------------|-----------------------|-----------------------|
| 5.94        | 5698                 | A''      | 18a'5a''                 | -28.2                 | -23.7                 | -29.8                 |
| 6.67        | 107 465              | A'       | 4a''5a'' - 3a''5a''      | -27.8                 | -25.2                 | -27.5                 |
| 6.79        | 63024                | A'       | 3a''5a'' + 4a''5a''      | -29.9                 | -24.9                 | -28.7                 |
| 7.12        | 6501                 | A''      | 17a'5a'' + 18a'6a''      | -27.0                 | -25.2                 | -29.4                 |
| 7.61        | 0 <sup>d</sup>       | A''      | 18a'6a'' - 17a'5a''      | -27.0                 | -26.0                 | -29.5                 |
| 7.61        | 627                  | A''      | 4a''19a'                 | -37.8                 | -31.2                 | -33.5                 |
| 7.72        | 7596                 | A'       | 18a'19a'                 | -28.8                 | -26.8                 | -28.8                 |
| 7.81        | 1046                 | A''      | 3a''21a'                 | -39.1                 | -40.4                 | -30.9                 |
| 7.84        | 9469                 | A'       | 4a''9a'' - 4a''7a''      | -34.2                 | -40.2                 | -32.8                 |
| 7.96        | 439445               | A'       | 4a''6a'' - 3a''5a''      | -38.3                 | -33.0                 | -33.3                 |
| 8.21        | 13341                | A''      | 3a''19a'                 | -37.3                 | -33.6                 | -33.4                 |
| 8.37        | 17366                | A''      | 4a''21a'                 | -36.5                 | -43.4                 | -31.0                 |
| 8.62        | 6374                 | A''      | 4a''20a'                 | -38.1                 | -44.1                 | -32.2                 |
| 8.65        | 8851                 | A''      | 17a'6a'' - 17a'5a''      | -27.8                 | -27.9                 | -31.2                 |
| 8.80        | 5                    | A''      | 3a''20a'                 | -37.1                 | -47.3                 | -31.4                 |
| 8.89        | 12731                | A'       | 18a'21a'                 | -29.9                 | -31.3                 | -34.2                 |
| 8.97        | 3934                 | A''      | 4a''22a'                 | -34.9                 | -44.3                 | -30.6                 |
| 9.21        | 10001                | A'       | 4a''8a'' + 3a''7a''      | -31.8                 | -38.0                 | -37.2                 |
| 9.22        | 2731                 | A''      | 16a'5a''                 | -28.5                 | -22.6                 | -30.4                 |
| 9.33        | 90023                | A'       | 3a''6a'' + 4a''7a''      | -30.1                 | -31.1                 | -35.8                 |
| 9.42        | 134                  | A''      | 4a''24a'                 | -35.0                 | -39.4                 | -29.7                 |
| 9.70        | 19094                | A'       | 3a''7a'' - 3a''5a''      | -34.1                 | -35.7                 | -35.1                 |
| 10.12       | 857                  | A''      | 18a'7a'' - 18a'5a''      | -27.4                 | -33.9                 | -41.0                 |
| 10.14       | 5460                 | A''      | 18a'9a''                 | -34.0                 | -33.2                 | -36.8                 |
| 10.63       | 5565                 | A'       | 18a'20a' - 17a'19a'      | -28.5                 | -38.5                 | -40.6                 |
| 10.76       | 30179                | A'       | 4a''8a'' + 4a''9a''      | -37.4                 | -38.5                 | -32.6                 |

<sup>a</sup>Basis sets (C,N/H [7s4p3d/4s2p2d]).

<sup>b</sup>Orbital occupancy 1-18a' 1-4a''; active MOs 7 - 174.

<sup>c</sup>Excitation energies are relative to the  $\tilde{X}^1A'$  ground state CI energy -281.63487 a.u.

<sup>d</sup>Accidental cancellation of contributions.

acter of low-lying valence and Rydberg states are listed in Tables II and III, respectively. Because of the complexity of the UPS Band 1 structure (Fig. 4(b)), the search for Rydberg states requires analysis of the VUV spectrum in considerable detail, as presented in Sec. IV above. Furthermore, the calculated intensities for some of the low lying Rydberg states (Table III), such as the S, X, and Y states, suggest that these will be very weak, and difficult to identify in the experimental spectrum.

### A. The energy region up to 7.2 eV

The experimental VUV photoabsorption spectrum of *1Me124T* (see Fig. 7) shows an initial onset near 5.75 eV rising to about 6.3 eV, where the VUV becomes an undulating plateau with shallow maxima up to 7.15 eV. Table II lists the vertical singlet excited states expected in this region. Two  $LP_N\pi^*$  states are calculated at 5.94 eV and 7.12 eV and two  $\pi\pi^*$  states calculated at 6.67 eV and 6.79 eV, leading to the calculated sequence of vertical singlet excited states as  $1^1A' < 1^2A' < 2^2A' < 2^2A''$ . These states correspond primarily to excitation from the four highest occupied orbitals of the molecule to the lowest unoccupied  $\pi^*$  orbital ( $5a''$ , Fig. S5); this is shown by the leading terms in Table II. The energies

TABLE III. Selected singlet Rydberg states for 1-methyl-1,2,4-triazole; vertical excitation energies (eV), oscillator strengths, and second moments (a.u.).<sup>a,b,c</sup>

| Energy/eV | $10^6 f(r)$ | Symmetry | Leading configuration | $\langle x^2 \rangle$ | $\langle y^2 \rangle$ | $\langle z^2 \rangle$ |
|-----------|-------------|----------|-----------------------|-----------------------|-----------------------|-----------------------|
| 7.54      | 156         | A''      | 4a''S                 | -76.9                 | -93.9                 | -66.9                 |
| 8.20      | 2224        | A''      | 3a''S                 | -75.0                 | -89.6                 | -65.1                 |
| 8.22      | 512         | A'       | 4a''(XZ+YZ)           | -69.0                 | -75.2                 | -121.5                |
| 8.22      | 2084        | A'       | 4a''Z                 | -54.7                 | -57.8                 | -107.0                |
| 8.39      | 266         | A''      | 4a''(X,Y)             | -149.7                | -100.7                | -51.5                 |
| 8.50      | 66          | A'       | 4a''(ZZ-XX-YY)Z       | -133.0                | -127.0                | -135.3                |
| 8.51      | 83          | A''      | 4a''(XZ+YZ)           | -171.0                | -173.8                | -214.8                |
| 8.70      | 820         | A''      | 4a''(XX-YY)           | -45.6                 | -54.7                 | -95.5                 |
| 8.71      | 132         | A''      | 4a''XY                | -213.1                | -210.2                | -145.0                |
| 8.73      | 9866        | A'       | 3a''Z                 | -50.0                 | -49.5                 | -94.2                 |
| 8.83      | 11          | A''      | 4a''S                 | -198.2                | -235.1                | -169.1                |
| 8.91      | 9091        | A''      | 4a''(X,Y)             | -79.8                 | -68.4                 | -54.2                 |
| 8.94      | 934         | A'       | 4a''XYZ               | -272.0                | -203.2                | -249.0                |
| 9.00      | 581         | A''      | 4a''(YY-ZZ)X          | -107.5                | -133.2                | -127.4                |
| 9.05      | 109         | A'       | 4a''(ZZ-XX-YY)Z       | -197.7                | -228.1                | -302.1                |
| 9.06      | 68          | A'       | 3a''XYZ               | -272.1                | -202.5                | -248.9                |
| 9.07      | 3341        | A''      | 4a''(XX-ZZ)Y          | -165.1                | -153.2                | -104.6                |
| 9.09      | 502         | A''      | 3a''(X,Y)             | -150.3                | -99.2                 | -55.4                 |
| 9.11      | 2           | A'       | 3a''(ZZ-XX-YY)Z       | -200.2                | -227.2                | -303.6                |
| 9.12      | 1172        | A''      | 3a''(XZ+YZ)           | -104.3                | -104.5                | -113.8                |
| 9.14      | 33          | A''      | 4a''S                 | -169.3                | -87.6                 | -124.8                |
| 9.16      | 6939        | A'       | 4a''(XZ+YZ)           | -125.0                | -208.8                | -280.2                |
| 9.22      | 5832        | A''      | 3a''(XX-YY)           | -46.2                 | -54.5                 | -96.0                 |
| 9.29      | 1           | A''      | 4a''(YY-XX-ZZ)Y       | -193.9                | -240.8                | -247.2                |
| 9.29      | 215         | A''      | 4a''XY                | -77.1                 | -74.8                 | -61.0                 |
| 9.49      | 668         | A''      | 3a''S                 | -200.6                | -237.5                | -171.0                |
| 9.51      | 22          | A''      | 4a''S                 | -548.8                | -539.4                | -555.5                |

<sup>a</sup>Contracted orbital basis sets (C,N/H [5s3p3d1f/3s3p2d] + Rydberg [4s3p3d3f]; total Cartesian GTOs 433, harmonic GTOs 375).

<sup>b</sup>Ground state SCF orbital occupancy 1-18a' 1-4a''; CI active MOs 7-222.

<sup>c</sup>Excitation energies are relative to the  $\tilde{X}^1A'$  ground state CI energy -280.62027 a.u.

of these states are depicted by the bars overlaid on the experimental spectrum in Fig. 5.

The two  $\pi\pi^*$  states, shown by the blue bars between 6.5 and 7 eV in Fig. 5, are the coupled pair of states discussed in Sec. III A 3, which behave as the pseudo degenerate pair  $1^1A'$  ( $4a''5a''-3a''5a''$ ) and  $2^1A'$  ( $3a''5a''+4a''5a''$ ). Since the latter undergoes distortion to a significantly non-planar structure ( $1^1A$ , in Fig. S4), the splitting of these two states is likely

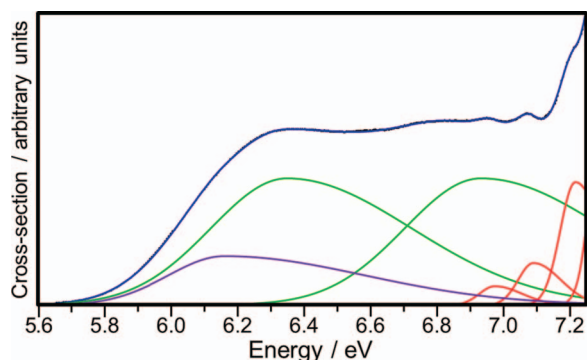


FIG. 7. The low-energy region of the VUV spectrum for **1Me124T** with a superimposed model of the excitations in this region (see text for explanation of the individual colored bands). The data are plotted as black points, but the overlaid blue fit line almost completely covers the data points.

to be greater than that depicted for the vertical states shown in Fig. 5; further, the coupling may also cause the excitations to the two states to have more similar band intensities and shapes.

The corresponding  $LP_N$  excitations also occur in linear combinations,  $17a'5a'' + 18a'6a''$  and  $18a'6a'' - 17a'5a''$  (Table III). However, there is a fundamental difference between these two states, since the latter is calculated to have zero oscillator strength, the result of a cancellation of terms in the transition dipole terms of the MOs.

A model of the VUV spectrum in this region, based on these considerations, is shown by the colored lines overlaid on the experimental spectrum in Fig. 7. The coupled  $\pi\pi^*$  absorptions are represented by the two green bands constrained to have equal intensity and shape. The low-energy  $LP_N\pi^*$  transition is represented by the purple band; the lower intensity and absence of well resolved fine structure on the leading edge of the onset, is consistent with the lowest singlet state being largely an  $LP_{N4\pi^*}$  ( $18a'5a''$ ) valence excitation. The red narrow peaks (Fig. 7) also have been constrained to have equal areas; this avoids more variable parameters in the fit than justified by the data. There may be a further member of this progression around 6.8-6.85 eV, but the intensity is too low to be included in the "fit" functions. Adjacent red peaks have separations of  $970\text{ cm}^{-1}$  and  $1028\text{ cm}^{-1}$ .

These separations are marginally smaller than that of the UPS Band 1 (Fig. 4(b)), where the first vibrational 0-0 and 0-1 pair are separated by  $1200\text{ cm}^{-1}$ . Hence, the bands shown in red (Fig. 7) are unlikely to arise from the  $4a''3s$  Rydberg state. A more acceptable interpretation for the red peaks above  $6.97\text{ eV}$  in Fig. 7 is that these arise from the second  $LP_{N2}\pi^*$  state (Table III); the vibrational separation contrasts with that for the  $LP_{N4}\pi^*$  state by having well resolved vibrational structure, as discussed below.

In the model depicted in Fig. 7, the raw data (black dots) are almost completely obscured by the fit (blue line) throughout this region. Because of the overlap of excitations in this region, other models could also account well for the total absorption intensity. The exact energies and shapes of the individual bands in Fig. 7 are uncertain, but the quality of the fit shows the consistency between the data and the number and character of the calculated excitations in this region. Further analysis shows a very low intensity oscillatory pattern with  $E(0) = 6.669(1)$  and vibrational frequency  $(\Delta E) = 0.012(1)$  eV. This vibrational frequency is consistent with values from torsional modes of a valence state; the lowest anharmonic frequency for the preferred conformer of *1Me124T* is  $82\text{ cm}^{-1}$ , corresponding to an out-of-plane ( $A''$ ) bending mode and suggestive of non-planar structures for the excited states.

## B. The intermediate region from 7.2 to 9.2 eV

There is marked VUV intensity between 7.2 and 8.2 eV. Overlay of the first UPS band on the VUV spectrum in Fig. 8 appears to show a Rydberg state at  $7.31\text{ eV}$  ( $v = 0$  band), while the second VUV peak at  $7.46\text{ eV}$  is identified with the  $v = 1$  UPS vibrational level. This separation of  $0.15\text{ eV}$  confirms these bands as the lowest assignable Rydberg state, where the  $4a''3p$  state has  $\delta = 0.55$ , a fairly typical value. However, the second UPS vibrational level ( $v = 2$ ), marked by an arrow on Fig. 8, appears to be missing from the VUV spectrum. This observation can best be explained by an underlying (broad) valence state occurring near  $7.5\text{ eV}$ , raising the baseline with loss of this second vibrational peak. Indeed, a

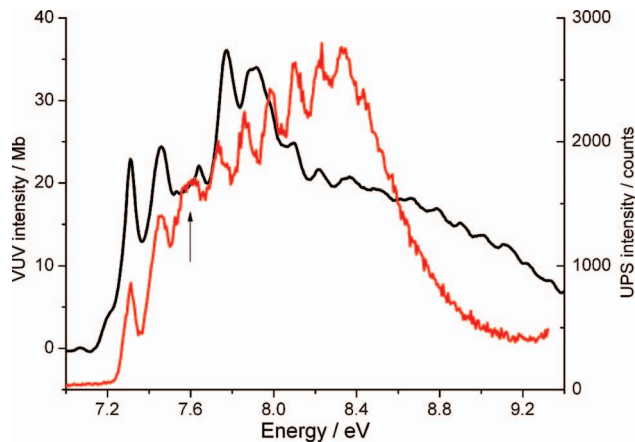


FIG. 8. Overlay of the UPS Band 1 spectrum (red) onto the VUV spectrum of *1Me124T* (black) to align the  $7.31\text{ eV}$  region. The arrow points to the major  $v = 2$  vibrational level in the UPS Band 1, which is apparently missing in the VUV spectrum.

group of five calculated valence states, including the strongest value for the spectrum, lies in the region  $7.6 - 8.0\text{ eV}$ , and it is reasonable to assign one or more of these as overwhelming the  $v = 2$  member.

The strongest peak in the spectrum is at  $7.77\text{ eV}$  (Fig. 8), with a double peak at  $7.89$  and  $7.92\text{ eV}$ . The first at  $7.77\text{ eV}$  suggests a further Rydberg state origin. If the state is related to  $IE_1$  at  $9.58\text{ eV}$ , the apparent  $\delta$  is  $0.258$  which seems too high for a  $3d$  state, and too low for a  $3p$  state. However, if the band origin is related to  $IE_2$ , using the present deconvoluted value of  $9.89\text{ eV}$ , we can attribute this to a  $3p$  state with  $\delta = 0.466$ ; the slightly smaller vibrational frequency for  $IE_2^A$  in the fit of Band 1 of the UPS, suggests that the line at  $7.89\text{ eV}$  is a vibrational satellite.

Similar considerations have been applied to the remaining spectrum. The strongest calculated valence states ( $7.96$  and  $9.33\text{ eV}$ ) must correlate with the other VUV peaks observed between  $7$  and  $10\text{ eV}$ . The four calculated  $\pi\pi^*$  electronic states with strongest intensity are all coupled and in each leading configuration, both  $3a''$  and  $4a''$  are prominent (Table III). This seems a further manifestation of an apparent near degeneracy of this pair of occupied MOs. Thus the calculated valence state at  $7.96\text{ eV}$  is the  $\pi\pi^*$  state with leading configuration  $4a''6a'' - 3a''5a''$ . No obvious assignments of this and other valence states to the present VUV spectrum are apparent.

Although some of the features starting at  $8.10\text{ eV}$  could be related to the lower VUV assignment at  $7.31\text{ eV}$ , it seems more probable that the continuing oscillations in cross section up to  $9.3\text{ eV}$  represent additional Rydberg states. Overlay of the VUV region between  $8.1$  and  $9.3\text{ eV}$  with Band 1 of the UPS (Fig. 9) shows a considerable number of coincidences, broadening in the VUV third maximum, and some broadening in the VUV  $8.3-8.4\text{ eV}$  maximum (Fig. 9). The overlay shown, whilst clearly not unique, does give good coincidences for several of the bands, but we conclude that the set of VUV maxima in Fig. 9 between  $8.1$  and  $9.3\text{ eV}$  cannot be a single progression. A comparison between the UPS and VUV spectra is simpler when the intrinsic slopes are removed from the two spectra to make the axes parallel; this allows a more

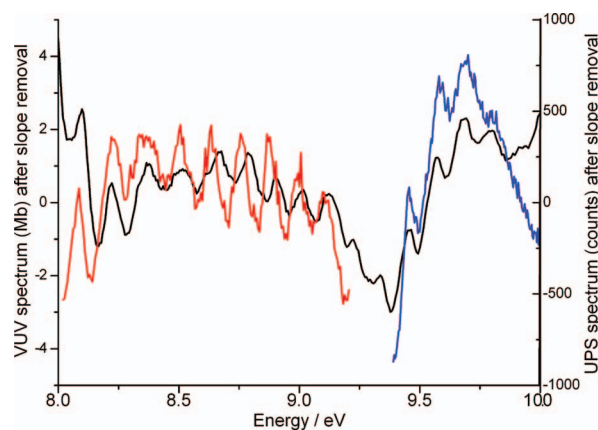


FIG. 9. Overlay of the UPS Band 1 spectrum (red) onto the VUV spectrum of *1Me124T* (black) for the  $8.0-9.3\text{ eV}$  region after flattening the UPS baseline, and overlay of the UPS Band 2 spectrum (blue) onto the VUV spectrum  $9.4-10.0\text{ eV}$  region.

complete overlay the UPS and VUV spectra. There is no exact match starting at either ends or the middle, since there are 11 VUV local maxima in the region of 8.10–9.34 eV, two more than in Band 1 of the UPS spectrum. Of course, some of this difference between the two techniques may arise from the potential curves of the excited states being shifted differently in each case. In this way, although many frequencies are largely preserved, the shifts are not identical. The present interpretation implies an  $IE_1$  4s Rydberg state with origin at 8.10 eV, while the residual peaks and shoulders starting at 8.38 eV are attributed to the corresponding  $IE_2$  4s state.

Further analysis of this region by a higher resolution technique such as multi-photon ionization (MPI) would be desirable; however, informal advice from practitioners of MPI is that the present  $IE_1$  and  $IE_2$  ionization energies could make this process difficult to achieve experimentally, especially in relation to both overlapping bands and lifetime issues.

### C. The region above 9.3 eV

The VUV spectrum shows weak fine structure continuing up to 11 eV, but generally, the spectrum declines in intensity with an undulating character, leading to a minimum just short of  $IE_1$  and  $IE_2$ . The well-resolved group of peaks with apparent 0-0 band at 9.45 eV (Fig. 9) relates to Band 2 ( $IE_4$ ) of the UPS (Fig. S6). The  $17a'$  3p-Rydberg state, with  $\delta = 0.50$ , a fairly typical 3p value, can be assigned to this VUV band. Interestingly, the relative intensities of the VUV and UPS spectra for this VUV energy range are opposite to those at lower VUV/UPS energy.

## VI. DISCUSSION

### A. The UPS results

The first band for each of these spectra (Fig. 4) is deceptively simple, where we find a declining separation of apparent vibrational peaks. When Band 1 of each molecule is analyzed in terms of the three ionizations thought to underlie the envelope, the fits obtained give apparent vibration frequencies of 1095 and 899  $\text{cm}^{-1}$  (*IH124T*) and 985 and 937  $\text{cm}^{-1}$  (*IMe124T*). The magnitudes of these fundamentals are similar to those found in pyrrole where they were assigned to skeletal stretching modes.<sup>47</sup> However, although the “fits” are relatively good, the variation in widths of individual peaks indicate that there are more than two vibrations in this band for each molecule. The four frequencies above are merely composites of several vibrational bands in each case, and the declining vibrational separations are explained on this basis. The UPS band shapes of both  $IE_3$  and  $IE_4$  are close to typical skewed Gaussians, and hence have very low 0-0 bands. This shape is often found in  $LP_N$  ionizations in the UPS of azines and azoles.<sup>51–54</sup>

### B. The VUV spectrum and valence states of *1Me124T*

The 1-methyl-derivative of *124T* proved a suitable alternative to *IH124T* that avoided any question of tautomeric composition, and with good vapor pressure gave the first

VUV spectral study of a member of the *124T* ring system. It disclosed a very complex profile, whose analysis was aided by experimental UPS spectra and electronic structure computations. Although much higher resolution is required for a complete analysis of both the UPS and VUV spectra, the present resolution is sufficient for interpretation of the main features. The present calculated valence states suggest that the lowest excited states all occupy the LUMO ( $5a''$ ). The onset of UV absorption which is rather weak, indicating that the first excited state ( $1^1A''$ ) is an  $LP_{N4}$  excitation. This is followed by two rather stronger  $\pi\pi^*$  states, and the second  $LP_{N2}$  excitation. The calculations suggest that all of the  $\pi\sigma^*$  and  $\sigma\pi^*$  states are very weak. Comparison with the excited states of *2HI23T*,<sup>3</sup> which also has two lone-pair orbitals, shows that the energy ranges are similar. In the *2HI23T* case, the lowest excited state is also an  $LP_{N\pi^*}$  state, the  $LP_N^-$  antisymmetric lone-pair combination ( $1^1A_2$ ). Whereas *2HI23T* shows four  $\pi\pi^*$  states with high oscillator strengths, all calculated to lie between 8.2 and 9 eV, *1Me124T* shows much weaker  $\pi\pi^*$  states, with apparently only two  $\pi\pi^*$  states at 8.0 ( $4a''6a'' - 3a''5a''$ ) and 9.3 eV ( $3a''6a'' + 4a''7a''$ ) contributing significantly to the intensity.

### C. The Rydberg states of *1Me124T*

The calculated energies of the Rydberg states (Table IV) suggest that a considerable density of states occurs in the region between 8 and 10 eV, making detailed assignment of this region of the VUV spectrum difficult. A small shift by 0.227 eV of the calculated set of Rydberg states (Table IV) based on the  $IE_1$  and  $IE_2$  excitations is sufficient to align with the first experimental Rydberg state (Fig. 7). When taken together with the valence states (Fig. 6), this demonstrates that much of the intensity between 7.5 and 8 eV is due to valence-state contributions. The principal Rydberg states identified, some of which are tentative given the low level of signal intensity above 10 eV, are shown in Table IV.

When the calculated excitation energy from different MOs into pairs of Rydberg states with the same upper state

TABLE IV. Rydberg states for 1-methyl-1,2,4-triazole, where those above 10 eV are tentative.

| Energy (eV) | Term value (eV) | Probable PQN ( $n$ ) | Probable QD ( $\delta$ ) | $IE^n$ (n) | State  |
|-------------|-----------------|----------------------|--------------------------|------------|--------|
| 7.09        | 2.48            | 3                    | 0.65                     | 1          | 3s     |
| 7.31        | 2.26            | 3                    | 0.55                     | 1          | 3p     |
| 7.77        | 1.80            | 3                    | 0.25                     | 1          | 3p     |
| 7.77        | 2.00            | 3                    | 0.62                     | 2          | 3p'    |
| 8.09        | 1.48            | 4                    | 0.96                     | 1          | 4s     |
| 9.46        | 2.17            | 3                    | 0.50                     | 2          | 3p     |
| 8.22        | 1.35            | 4                    | 0.82                     | 1          | 4s     |
| 8.38        | 1.39            | 4                    | 0.88                     | 2          | 4s     |
| 9.45        | 2.70            | 3                    | 0.88                     | 4          | 3s     |
| 10.06       | 2.10            | 3                    | 0.45                     | 4          | 3p     |
| 10.16       | 1.99            | 3                    | 0.38                     | 4          | 3p'    |
| 10.53       | 1.62            | 3                    | 0.10                     | 4          | 3d     |
| 10.62       | 1.54            | 3(4)                 | 0.02(1.02)               | 4          | 3d(4s) |

type (i.e.,  $nS$ ,  $nP$ ,  $nD$ , or  $nF$ ) are compared, then we get an independent measure of the difference in energy of the bound MOs, as discussed in Sec. III B 1. For example, the  $4a''3S$  and  $3a''3S$  states have an energy difference of 0.66 eV. Although some exceptions occur, there is a relatively good linear correlation ( $R^2 = 0.961$ ) between the two sets of data involving the  $4a''$  and  $3a''$  MOs, with  $E_{4a''} = [0.89(6)E_{3a''} + 0.46(58)]$  eV. The median energy difference for excitations to a common upper state from these two MOs is 0.60 eV. This is relatively close to the IE<sup>A</sup> “fit” data and direct calculation of the differences in adiabatic IE, as discussed above, and is a further indication of internal consistency in the results obtained here.

## VII. CONCLUSIONS

The VUV spectrum of 1-methyl-1,2,4-triazole shows a number of unusual features. The VUV onset region shows a near plateau in cross section between 6 and 7 eV, and has been analyzed in terms of four valence states, notionally two  $\pi\pi^*$  and two  $LP_N$ , but it seems clear from the theoretical studies of singlet excited states that some of the lowest  $\pi\pi^*$  states become non-planar. The vertical excited Rydberg state calculations suggest that a dense packing of such states occurs in the 8–9 eV energy region; several relating to the first, second, and fourth ionization processes have been identified. The failure to identify Rydberg states derived from IE<sub>3</sub> must be related to the broad Gaussian band attributed to this ionization. IE<sub>4</sub> has a simple well-defined structure, which makes spectral identification relatively straightforward. The improvements in the UV photoelectron spectra quality obtained here for both *IH124T* and *IMe124T* are critical for the assignment of these Rydberg states. Most of the calculated Rydberg states are predicted to have very low oscillator strengths, and the VUV spectrum appears to be more dominated by valence states.

In these states, the methyl group tilts from the ring plane, but the ring H-C bonds seem equally prone to rotation out of plane. This contrasts with the first lone-pair excitation,  $18a'5a''$  ( $1^1A''$ ), where the planar form seems certain. The linear combinations of lone-pairs have an energy separation of about 1.5 eV, and while the lowest state (dominated by  $LP_{N4}$ ) shows no vibrational structure, the higher energy state (dominated by  $LP_{N2}$ ) appears to show two or more vibrational modes. In both the singlet and cationic manifolds, non-planarity is a major issue. Although the global equilibrium structure for the first cation is effectively planar, the second ionization shows significant twisting of the ring system. The conventional wisdom<sup>51–54</sup> from most studies of conjugated “aromatic molecules” such as the azines and azoles, is that the cations observed in the UPS are planar as a result of the “aromatic” character. In the light of the present study of *IMe124T* and previously *2IH123T*,<sup>3</sup> reconsideration of this point may be well rewarded.

## ACKNOWLEDGMENTS

M.H.P. and P.J.C. thank the UK National Grid Service (NGS) Operations Support Centre and National Service for Computational Chemistry Software (NSCCS) for computing support, and Dr. P. Sherwood (Daresbury Laboratory) for

maintenance of the GAMESS-UK suite of programmes. D.L.L. thanks the National Science Foundation (NSF) through the Project No. CHE-0749530. We thank Elliott Smith for the collection of the UPS data of *IH124T*, Dr. R. A. Aitken (School of Chemistry, University of St. Andrews) for the synthesis of the *IMe124T* sample. A.R.H. thanks the Department of Chemistry and Biochemistry, The University of Arizona, for support of the Molecular Photoelectron Spectroscopy facility.

- <sup>1</sup>D. S. Bele and I. Singhvi, *Asian J. Biochem. Pharm. Res.* **1**, 88 (2011).
- <sup>2</sup>S. W. Kim, A. Biegón, Z. E. Katsamanis, C. W. Ehrlich, J. M. Hooker, C. Shea, L. Muench, Y. Xu, P. King, P. Carter, D. L. Alexoff, and J. S. Fowler, *Nucl. Med. Biol.* **36**, 323 (2009).
- <sup>3</sup>M. H. Palmer, S. V. Hoffmann, N. C. Jones, A. R. Head, and D. L. Lichtenberger, *J. Chem. Phys.* **134**, 084309 (2011).
- <sup>4</sup>M. H. Palmer, I. Simpson, and J. R. Wheeler, *Z. Naturforsch.* **36A**, 1246 (1981).
- <sup>5</sup>G. Herzberg, *Molecular Spectra and Molecular Structure 1: Spectra of Diatomic Molecules*, reprinted with corrections (Krieger, Malabar, Florida, USA, 1989).
- <sup>6</sup>G. Herzberg, *Molecular Spectra and Molecular Structure 3: Electronic Spectra and Electronic Structure of Polyatomic Molecules*, reprinted with corrections (Krieger, Malabar, Florida, USA, 1991).
- <sup>7</sup>C. F. Dion and E. R. Bernstein, *J. Chem. Phys.* **103**, 4907 (1995).
- <sup>8</sup>E. Miescher and K. P. Huber *International Review of Science, Physical Chemistry Series*, edited by D. A. Ramsay, *Series 2* (Butterworths, London, 1976), Vol. 3, pp. 37–73.
- <sup>9</sup>J. G. Philis, T. Mondal, and S. Mahapatra, *Chem. Phys. Lett.* **495**, 187 (2010).
- <sup>10</sup>D. M. P. Holland, D. A. Shaw, M. Stener, and P. Decleva, *J. Phys. B* **42**, 245201 (2009).
- <sup>11</sup>V. A. Shubert, M. Rednic, and S. T. Pratt, *J. Chem. Phys.* **132**, 124108 (2010).
- <sup>12</sup>J. Pitarch-Ruiz, A. Sánchez de Merás, J. Sánchez-Marín, A. M. Velasco, C. Lavín, and I. Martín, *J. Phys. Chem. A* **112**, 3275 (2008).
- <sup>13</sup>D. E. Love and K. D. Jordan, *J. Phys. Chem. A* **103**, 5667 (1999).
- <sup>14</sup>H. Lefebvre-Brion, H. P. Liebermann, and G. J. Vazquez, *J. Chem. Phys.* **134**, 204104 (2011).
- <sup>15</sup>M. P. Minitti, J. D. Cardoza, and P. M. Weber, *J. Phys. Chem. A* **110**, 10212 (2006).
- <sup>16</sup>D. P. Seccombe, R. P. Tuckett, H. Baumgärtel, and H. W. Jochims, *Phys. Chem. Chem. Phys.* **1**, 773 (1999).
- <sup>17</sup>H. Meyer, *J. Chem. Phys.* **107**, 7721 (1997).
- <sup>18</sup>H. Meyer, *J. Chem. Phys.* **107**, 7732 (1997).
- <sup>19</sup>I. Ciofini and C. Adamo, *J. Phys. Chem. A* **111**, 5549 (2007).
- <sup>20</sup>A. M. Velasco, J. Pitarch-Ruiz, A. M. J. Sánchez de Merás, J. Sánchez-Marín, and I. Martín, *J. Chem. Phys.* **124**, 124313 (2006).
- <sup>21</sup>M. Warken, *J. Chem. Phys.* **103**, 5554 (1995).
- <sup>22</sup>K. Bolton, R. D. Brown, F. R. Burden, and A. Mishra, *J. Chem. Soc., Chem. Commun.* **1971**, 873.
- <sup>23</sup>K. Bolton, R. D. Brown, F. R. Burden, and A. Mishra, *J. Mol. Spectrosc.* **57**, 294 (1975).
- <sup>24</sup>K. Bolton, R. D. Brown, F. R. Burden, and A. Mishra, *J. Mol. Struct.* **27**, 261 (1975).
- <sup>25</sup>J. F. Chiang and K. C. Lu, *J. Mol. Struct.: THEOCHEM* **41**, 223 (1977).
- <sup>26</sup>M. H. Palmer and A. J. Beveridge, *Chem. Phys.* **111**, 249 (1987).
- <sup>27</sup>See supplementary material at <http://dx.doi.org/10.1063/1.3692164> for additional material relating to (a) the sample characterization and the spectroscopic methods; (b) the computational techniques for finding minimum energy structures and the planar and non-planar cationic and singlet state structures of *IMe124T*; (c) the methodology for the UPS Band 2 fitting process and the final “fitting” parameters for the UPS Band 1 and Band 2 of *IH124T* and *IMe124T*; (d) the most important MOs of *IMe124T* contributing to the present UPS and VUV study; (e) expansion of UPS Band 2 for both compounds; (f) superposition of calculated vibrational states on UPS; and (g) the main *IH124T* and *IMe124T* ionization energies compared with calculated values.
- <sup>28</sup>K. Siegbahn, C. Nordling, A. Fahlman, R. Nordberg, K. Hamrin, J. Hedman, G. Johansson, T. Bergmark, S. E. Karlsson, I. Lindgren, and B. Lindberg, *Nova Acta Regiae Soc. Sci. Ups.* **20**, 282 (1967).

- <sup>29</sup>M. A. Cranswick, A. Dawson, J. J. A. Cooney, N. E. Gruhn, D. L. Lichtenberger, and J. H. Enemark, *Inorg. Chem.* **46**, 10639 (2007).
- <sup>30</sup>D. L. Lichtenberger, G. E. Kellogg, J. G. Kristofzski, D. Page, S. Turner, G. Klinger, and J. Lorenzen, *Rev. Sci. Instrum.* **57**, 2366 (1986).
- <sup>31</sup>M. F. Guest, I. J. Bush, H. J. J. Van Dam, P. Sherwood, J. M. H. Thomas, J. H. Van Lenthe, R. W. A. Havenith, and J. Kendrick, *Mol. Phys.* **103**, 719 (2005).
- <sup>32</sup>M. J. Frisch, G. W. Trucks, H. B. Schlegel *et al.*, GAUSSIAN 09, Revision A.02, Gaussian, Inc., Wallingford, CT, 2009.
- <sup>33</sup>F. Aquilante, L. De Vico, N. Ferré, G. Ghigo, P.-Å. Malmqvist, P. Neogady, T. B. Pedersen, M. Pitonak, M. Reiher, B. O. Roos, L. Serrano-Andrés, M. Urban, V. Veryazov, and R. Lindh, *J. Comput. Chem.* **31**, 224 (2010) for MOLCAS 7.6.
- <sup>34</sup>V. Veryazov, P.-O. Widmark, L. Serrano-Andrés, R. Lindh, and B. O. Roos, *Int. J. Quantum Chem.* **100**, 626 (2004) for MOLCAS code development.
- <sup>35</sup>D. E. Woon and T. H. Dunning, *J. Chem. Phys.* **100**, 2975 (1994).
- <sup>36</sup>M. H. Palmer, G. Ganzenmüller, and I. C. Walker, *Chem. Phys.* **334**, 154 (2007).
- <sup>37</sup>R. Ahlrichs and P. R. Taylor, *J. Chim. Phys. Phys.-Chim. Biol.* **78**, 315 (1981).
- <sup>38</sup>Origin V8.5.OSR1 (OriginLab, Northampton, MA); <http://www.Originlab.com>.
- <sup>39</sup>T. Williams, C. Kelley, H.-B. Broeker, J. Campbell, R. Cunningham, D. Denholm, G. Elber, R. Fearick, C. Grammes, L. Hart, L. Hecking, T. Koenig, D. Kotz, E. Kubaitis, R. Lang, T. Lecomte, A. Lehmann, A. Mai, E. A. Merritt, P. Mikulik, C. Steger, T. Tkacik, J. Van der Woude, A. Woo, J. R. Van Zandt, and J. Zellner, GNUPLOT 4.5: An interactive plotting program; see also <http://www.gnuplot.info>.
- <sup>40</sup>W. Humphrey, A. Dalke, and K. Schulten, *J. Mol. Graphics* **14**, 33 (1996). See also <http://www.ks.uiuc.edu/Research/vmd/>.
- <sup>41</sup>R. J. Buenker and R. A. Phillips, *J. Mol. Struct.:THEOCHEM* **24**, 291 (1985).
- <sup>42</sup>R. J. Buenker, *Current Aspects of Quantum Chemistry*, edited by R. Carbó (Elsevier, New York, 1982), Vol. 21, pp. 17–21.
- <sup>43</sup>R. J. Buenker and S. Krebs, “The configuration-driven approach for multireference configuration interaction calculations,” in *Recent Advances in Multireference Methods*, edited by K. Hirao (World Scientific, Singapore, 1999), pp. 1–29.
- <sup>44</sup>S. Huber, T.-K. Ha, and A. Bauder, *J. Mol. Struct.* **413-414**, 93 (1997).
- <sup>45</sup>S. Ohta, I. Kawasaki, A. Fukuno, M. Yamashita, T. Tada, and T. Kawabata, *Chem. Pharm. Bull. (Tokyo)* **41**, 1226 (1993).
- <sup>46</sup>S. Craddock, R. H. Findlay, and M. H. Palmer, *Tetrahedron* **29**, 2173 (1973).
- <sup>47</sup>L. S. Cederbaum, W. Domcke, J. Schirmer, W. von Niessen, G. H. F. Diercks, and W. P. Kraemer, *J. Chem. Phys.* **69**, 1591 (1978).
- <sup>48</sup>M. H. Palmer, A. J. Gaskell, and R. H. Findlay, *J. Chem. Soc., Perkin Trans. 1* **2**, 778 (1974).
- <sup>49</sup>M. Malagoli, V. Coropceanu, D. A. de Silva Filho, and J. L. Brédas, *J. Chem. Phys.* **120**, 7490 (2004).
- <sup>50</sup>S. Bonness, B. Kirtman, M. Huix, A. J. Sanchez, and J. M. Luis, *J. Chem. Phys.* **125**, 014311 (2006).
- <sup>51</sup>P. J. Derrick, L. Asbrink, Ö. Edqvist, and E. Lindholm, *Spectrochim. Acta* **27A**, 2525 (1971).
- <sup>52</sup>E. Heilbronner, J. P. Maier, and E. Haselbach, “UV photoelectron spectra of heterocyclic compounds” in *Physical Methods in Heterocyclic Chemistry*, edited by A. R. Katritzky (Academic, New York, 1974), pp. 1–52.
- <sup>53</sup>L. Asbrink, C. Fridh, B. Ö. Johnsson, and E. Lindholm, *Int. J. Mass Spectrom. Ion Phys.* **8**, 215 (1972).
- <sup>54</sup>L. Asbrink, C. Fridh, B. Ö. Johnsson, and E. Lindholm, *Int. J. Mass Spectrom. Ion Phys.* **8**, 229 (1972).